CHIN. PHYS. LETT. Vol. 31, No. 5 (2014) 055202

Spectroscopic Diagnostics of Atmospheric Argon Microwave Plasma Based on an Inductive Coupling Window-Rectangular Resonator

WANG Zhong(王仲)**, ZHANG Gui-Xin(张贵新), LIU Cheng(刘程), JIA Zhi-Dong(贾志东)

Department of Electrical Engineering, Tsinghua University, Beijing 100084

(Received 23 December 2013)

We present a novel microwave plasma source based on an inductive coupling window-rectangular resonator. A definite volume of atmospheric argon microwave plasma is excited in the source under the input of several kilowatts of microwave power operating at 2.45 GHz. The excitation temperature and electron temperature of the argon plasma are separately researched by using Boltzmann plot and line-to continuum intensity ratio of Ar I spectral lines. Its electron density is inferred from the Stark broadening of the H_β line at 486.13 nm.

PACS: 52.80.Pi, 52.50.Dg, 52.70.Kz DOI: 10.1088/0256-307X/31/5/055202

Microwave plasma has been widely applied to lots of industrial fields due to its advantages over other plasmas. Large-volume stable atmospheric microwave plasmas are preferential in these applications. A novel microwave plasma source based on an inductive coupling window-rectangular resonator is developed in this work. Also, the excitation temperature $T_{\rm exc}$, electron temperature $T_{\rm e}$ and electron density $n_{\rm e}$ of the atmospheric argon microwave plasma driven by the plasma source are deeply researched.

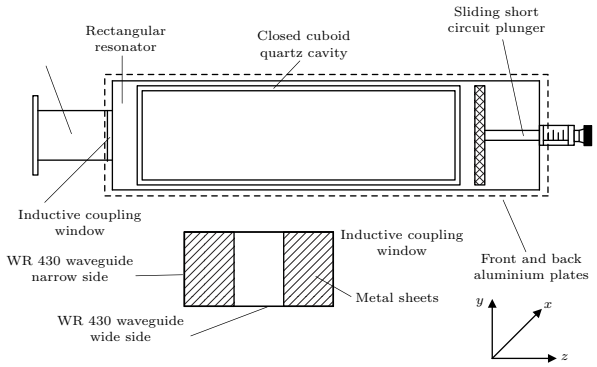


Fig. 1. Structure diagram of the microwave plasma source.

Figures 1 and 2 separately show the structure diagram and picture of the microwave plasma source. It consists of a WR430 waveguide, an inductive coupling window, a rectangular resonator, a closed cuboid quartz cavity and a sliding shorting plunger. In fact, the inductive coupling window is formed by inserting a metal sheet through each of the waveguide narrow walls. The rectangular resonator is composed of several metal plates including front and back aluminium plates, which serve as its narrow walls. The quartz cavity is equipped in the rectangular resonator. There is a quartz breather tube in each of the narrow walls of the quartz cavity. The breather tubes as the gas inlet and outlet go through the through-holes (ϕ = 20 mm, e.g., A in Fig. 2) in the front and back aluminium plates. The shorting plunger is used to adjust the resonator length. All the metallic materials of the microwave plasma source are of aluminum. The microwaves couple into the rectangular resonator through the coupling window. A resonance may be formed in the resonator by adjusting the plunger. Thus, the strong electric field in the quartz cavity caused by the resonance maybe makes the production of a large-volume stable atmospheric microwave plasmas possible. The structure and dimensions of the microwave plasma source are optimized by calculating the electric intensity in the resonator by using the software CST (Computer Simulation Technology). In the calculation, the relative permittivity and the relative permeability of the quartz are separately set as 3.78 and 1. The optimized results indicate: the width, height and thickness of the coupling window are 35.5 mm, 54.61 mm and 2 mm, respectively; the sizes of the internal cross section of the resonator are 113.22 mm × 77 mm; the inside sizes of the cuboid quartz cavity are 224 mm × 96 mm × 60 mm, and the wall thickness is 8 mm; the sliding range of the shorting plunger is 0 ∼90 mm; the electric intensity in the quartz cavity maximizes as the resonator length is 260 mm.

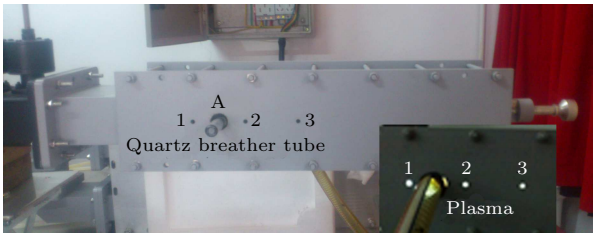


Fig. 2. Picture of the microwave plasma source.

The atmospheric argon microwave plasma initiated by the microwave plasma source is also shown in Fig. 2. The excitation power and extinguish power of the plasma are roughly 2.6 kW and 2.0 kW operating at 2.45 GHz, respectively. The plasma can be observed through the holes 1 and 2 (diameter = 5 mm) in the front aluminium plate. The distance between the

**Corresponding author. Email: zhongwang1986@126.com

© 2014 Chinese Physical Society and IOP Publishing Ltd

holes 1 and 2 is about 63 mm, which indicates that the plasma size is at least 63 mm in the length direction of the resonator. The root of the plasma is found to be located at the inside of the quartz cavity wide wall, and the holes 1 and 2 are both 30 mm away from the wall inside, which illustrates that the plasma size is at least 30 mm in the height direction of the resonator.

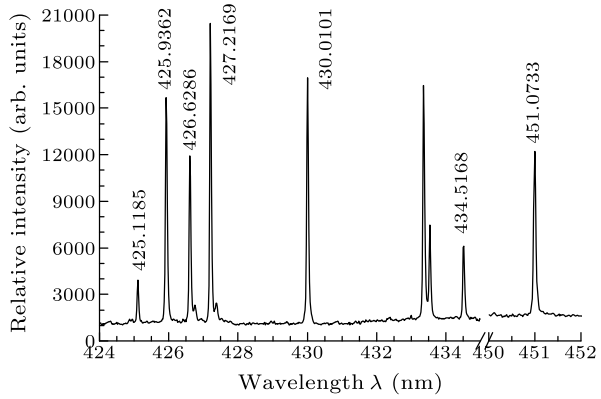


Fig. 3. Ar I spectral lines of the atmospheric argon plasma.

A Princeton instrument monochromator (Acton SP 2500, 0.500 m focal length, 1200 grooves/mm, blazed at 750 nm) connected to a CCD detector (Pixis 1024 × 1024) is used to acquire the atomic emission spectra of the atmospheric argon microwave plasma. The resolution of the whole optical measurement system is about 0.02 nm. The entrance slit of the monochromator is set as 10 μm in the measurement of the excitation and electron temperatures to acquire argon atomic spectral lines with good resolution performance while that 40 μm in the measurement of the electron density to reduce the influence of the low optical resolution on the line profile of the H_β (486.13 nm) spectral line. Figure 3 shows a part of the Ar I spectral lines of the atmospheric argon microwave plasma. The Ar I lines listed in Table 1 are applied to calculate the excitation temperature by using the Boltzmann plot[1]

$$\ln\frac{I_{\rm ul}\lambda_{\rm ul}}{g_{\rm u}A_{\rm ul}} = -\frac{E_{\rm u}}{k_{\rm B}T_{\rm exc}} + \ln\frac{Nhlc}{4\pi Z(T_{\rm exc})}, \qquad (1)$$

where $g_{\rm u}$ and $E_{\rm u}$ are separately the statistical weight and energy level of the upper state of the transition $(u-l)$, $A_{\rm ul}$ is the transition probability, $\lambda_{\rm ul}$ is the central wavelength of the transition, $T_{\rm exc}$ is the excitation temperature, and $Z(T_{\rm exc})$ is the partition function of the atom.

Figure 4 gives an example of calculating the excitation temperature by using the Boltzmann plot. In the figure, the linear relationship between $\ln(I\lambda/gA)$ and $E_{\rm u}$ (the energy level $E_{\rm u}$ is relatively high and even approaches to the ionization energy 15.76 eV of an argon atom) still exists, which indicates that such higher levels remain Boltzmann in the distribution and at least the partial local thermal equilibrium (pLTE) is satisfied in the atmospheric argon microwave plasma.[3]

Table 1. Parameters of Ar I spectral lines.[2]

$\lambda_{\rm ul}$ (nm)	$A_{\rm ul}$ (10^6 s^{-1})	$E_{\rm u}$ (eV)	$g_{\rm u}$
425.1185	0.111	14.4639949	3
425.9362	3.98	14.7381144	1
426.6286	0.312	14.5289126	5
427.2169	0.797	14.5249124	3
430.0101	0.377	14.5060667	5
433.3561	0.568	14.6882894	5
433.5338	0.387	14.6871173	3
434.5168	0.297	14.6806494	3
451.0733	1.18	14.5759479	1
487.6261	0.78	15.4489124	5
488.7947	1.3	15.4428352	3
506.0079	0.37	15.5252741	9
518.7746	1.38	15.2962923	5
522.1271	0.88	15.4496521	9
542.1352	0.6	15.3620404	5
545.1652	0.47	15.1806326	5
549.5874	1.69	15.3310391	9
555.8702	1.42	15.1368475	5
560.6733	2.2	15.1177454	3
565.0704	3.2	15.1005428	1

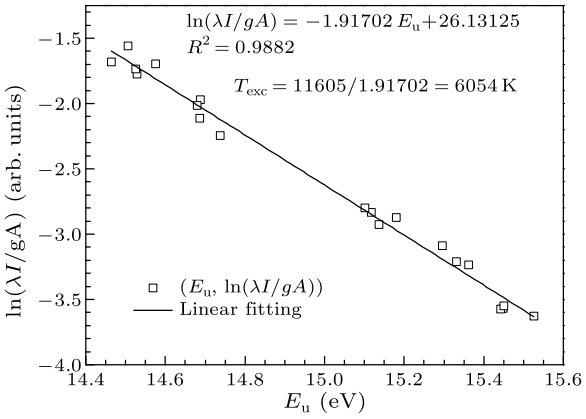


Fig. 4. An example of Boltzmann plot.

The line-to-continuum intensity ratio ($I_{\rm ul}/\varepsilon_{\rm c}$, in units of nm) expressed by Eq. (2) is usually applied to calculate the electron temperature.[3,4] In the expression, $I_{\rm ul}$ is the integration of the corresponding emission coefficient $\varepsilon_{\rm ul}$ over the spectral profile of the considered line $(u-l)$ with the central wavelength $\lambda_{\rm ul}$. The continuum emission coefficient $\varepsilon_{\rm c}$ results from the sum of two contributions: one is attributed to the capture of an electron by an ion, corresponding to the free-bound continuum (namely recombination continuum) with the emission coefficient $\varepsilon_{\rm fb}$; the other one is due to the interaction between an electron and the electric field of an ion or atom, corresponding to the free-free continuum (namely bremsstrahlung) with the emission coefficient $\varepsilon_{\rm ff}$, which is the sum of $\varepsilon_{{\rm ff},z>1}$ associated with an ion and $\varepsilon_{{\rm ff},z=1}$ linked to an atom. For practical use, $\varepsilon_{{\rm ff},z=1}$ is generally neglected even under the condition that the electron temperature and electron density are separately in the range from 5000 K to 10000 K and from 10^{14} cm^{-3} to 10^{15} cm^{-3},[3,4] in which the parameters of our plasma are just. That is to say, $\varepsilon_{\rm c}$ in Eq. (2) is actually the sum of $\varepsilon_{\rm fb}$ and

$\varepsilon_{\mathrm{ff},z>1}$, exactly speaking $\varepsilon_{\mathrm{ff},z=2}$, namely the continuum emission coefficient related to the first ion or Ar^+ in this work ($z-1$ is the number of charge). Note that ε_c is the continuum emission coefficient extremely near the considered line $(u-l)$.

$$\frac{I_{\mathrm{ul}}}{\varepsilon_c} = \underbrace{\frac{3^{3/2}h^4c^3}{256\pi^3 k_B e^6}}_{C_r} \frac{g_u A_{\mathrm{ul}}}{Z_i}\frac{\lambda_{\mathrm{ul}}}{T_e} \cdot \exp\left(\frac{E_i-\Delta E_i}{k_B T_e} - \frac{E_u}{k_B T_{\mathrm{exc}}}\right) / \left(\xi_{\mathrm{fb}}\left(1-\exp\left(-\frac{hc}{\lambda_{\mathrm{ul}} k_B T_e}\right)\right) + g_{\mathrm{ff}} \exp\left(-\frac{hc}{\lambda_{\mathrm{ul}} k_B T_e}\right)\right), \quad (2)$$

where $C_r = 2.005\times10^{-5}$ K·s, g_u, A_{ul}, λ_{ul} and E_u are the same as those in Eq. (1), Z_i as a function of T_{exc} is the partition function of the first ion and it is generally considered to equal to the statistical weight of the ground state of the first ion at relatively low temperature ($<$ 15000 K), $Z_i \approx 5.5$ for Ar^+, E_i and ΔE_i are the ionization energy of the atom and the lowering of the ionization energy, respectively, $E_i = 2.525\times10^{-18}$ J and $\Delta E_i < 4\times10^{-22}$ J for an argon atom, both ξ_{fb} and g_{ff} as the complicated functions of λ and T_e are separately the free-bound Biberman factor and free-free Gaunt factor.

In Ref. [5] the authors gave the calculated Biberman factors ξ_{fb} for different wavelengths and electron temperatures. The values of ξ_{fb} at the wavelengths of the Ar I lines (see Fig. 3) all have no significant change with T_e from 5000 K to 10000 K, and the factors ξ_{fb} are all about 1.5, and the independence of ξ_{fb} on T_e is helpful to decrease the difficulty in calculating the unknown electron temperature. The Gaunt factor g_{ff} corresponding to Ar^+ ($z=2$) is expressed in the following by taking into account the non-classical behavior,[6–7]

$$g_{\mathrm{ff},z=2} = 1 + 0.1728\left(\frac{hc}{\lambda E_{\mathrm{H}}}\right)^{1/3}\left(1+\frac{2\lambda k_B T_e}{hc}\right), \quad (3)$$

where E_{H} is the ionization energy (13.60 eV) of the hydrogen atom. The factors g_{ff} of Ar^+ at the wavelengths of the Ar I lines (see Fig. 3) are calculated and the result shows that g_{ff}'s at all the considered wavelengths increase from 1.13 to 1.17 with T_e from 5000 K to 10000 K. Our calculation indicates that such increase in g_{ff} has no evident effect on the calculation result of T_e. Therefore, similar to ξ_{fb}, g_{ff} is fixed at 1.15 in the calculation of T_e.

Figure 5 is the dependences of the excitation temperature T_{exc} and electron temperature T_e corresponding to the Ar I lines marked in Fig. 3 on the input microwave power. Here T_{exc} is obtained by using the Boltzmann plot of Ar I line listed in Table 1, while T_e is a consequence of T_{exc} and $I_{\mathrm{ul}}/\varepsilon_c$ through Eq. (2). As can be seen in Fig. 5, T_{exc} approaches to T_e for every Ar I line, with a deviation of at most 400 K, which once again indicates that at least the pLTE situation exists in the atmospheric argon microwave plasma. The existence of the pLTE situation in the atmospheric argon microwave plasma is consistent with the results appearing in Ref. [3]. The electron temperatures for different Ar I lines are also extremely close. They both increase from 5000 K to 8000 K as the input microwave power increases from 3 kW to 8 kW considering the measurement uncertainty.

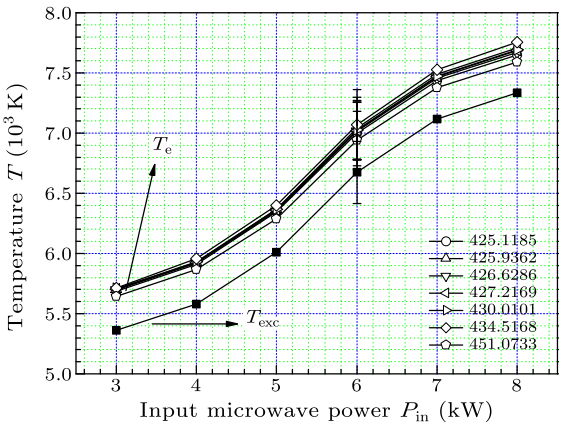


Fig. 5. Dependences of T_{exc} and T_e on the input power.

The Stark broadening of the well-known H_β spectral line at 486.13 nm is applied to calculate the electron density n_e of the atmospheric argon microwave plasma.[4] The H_β line profile is a Voigt profile as a consequence of the convolution between a Gaussian profile (instrumental broadening and Doppler broadening) and Lorentzian profile (Stark broadening, van der Waals broadening, resonance broadening and natural broadening). The Gaussian broadening expressed in full width at half maximum (FWHM, in units of nm) is the root of the sum of the squared instrumental broadening and Doppler broadening, and the Lorentzian broadening is the sum of the Stark broadening, van der Waals broadening, resonance broadening and natural broadening, and the latter two are generally omitted. Here we present the expressions of every broadening (FWHM, nm) of the H_β line (486.13 nm).[8,12]

$$\Delta\lambda_{\mathrm{Stark}}: \quad n_e = \left(\frac{1}{2}\Delta\lambda_{\mathrm{Stark}}\times10^{11}\right)^{1/0.668}, \quad (4)$$

$$n_e = 10^{16.578}(\Delta\lambda_{\mathrm{Stark}})^{1.478-0.144\log(\Delta\lambda_{\mathrm{Stark}})}T_e^{-0.1265}, \quad (5)$$

$$\Delta\lambda_{\text{van der Waals}}: \quad 5.521\times P/T_g^{0.7},$$

$$\Delta\lambda_{\mathrm{resonance}}: \quad 60.4\chi_{\mathrm{H}}(P/T_g),$$

$$\Delta\lambda_{\mathrm{natural}}: \quad 6.2\times10^{-5}\ \mathrm{nm},$$

$$\Delta\lambda_{\mathrm{Doppler}}: \quad 3.48\times10^{-4}T_g^{1/2},$$

$$\Delta\lambda_{\mathrm{instrumental}}: \quad 0.07348\ \mathrm{nm},$$

where P is the gas pressure (atm), T_g is the gas tem-

perature in units of K, and $\chi_{\rm H}$ is the mole fraction of hydrogen atoms.

The electron density $n_{\rm e}$ is concluded from the Stark broadening of the H_β line through Eqs. (4) and (5), separately quoted in Refs. [8,9]. The former including the ionic dynamic effect indicates that $n_{\rm e}$ is only dependent on $\Delta\lambda_{\rm Stark}$. The latter as an analytical expression from the tables given by Vidal *et al.*[10] shows that $n_{\rm e}$ is a function of $\Delta\lambda_{\rm Stark}$ and $T_{\rm e}$, the increase of which leads to the weak decrease of $n_{\rm e}$. The validity domain of Eq. (4) is $n_{\rm e} > 10^{14}\,{\rm cm}^{-3}$ and $T_{\rm e} > 1000\,{\rm K}$, while that of Eq. (5) is $3.16\times10^{14}\,{\rm cm}^{-3} < n_{\rm e} < 3.16\times10^{16}\,{\rm cm}^{-3}$ and $5000\,{\rm K} < T_{\rm e} < 20000\,{\rm K}$, in which $T_{\rm e}$ calculated through Eq. (5) has a deviation of $\pm5\%$ from the value in the tables in Ref. [10].

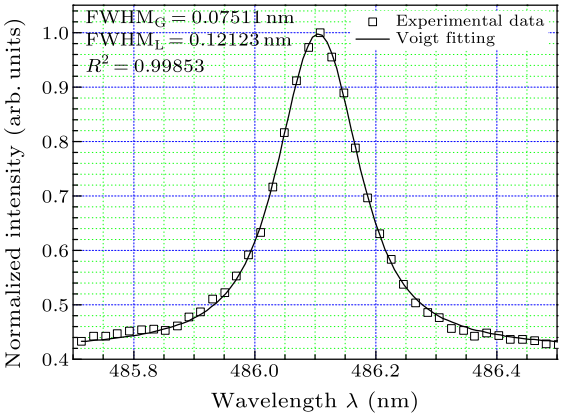


Fig. 6. An example of Voigt fitting of the H_β line.

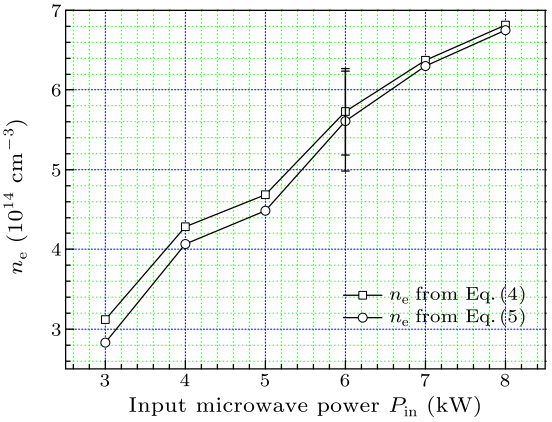


Fig. 7. Dependences of $n_{\rm e}$ on the input microwave power.

The instrumental broadening assimilated to a Gaussian profile is measured to be 0.07348 nm by using a He-Ne laser at 632.8 nm. It is found in our research that the gas temperature $T_{\rm g}$, nearly equals the rotational temperature $T_{\rm rot}$ determined by OH A-X rotation-vibration spectra,[11] is immune to the input microwave power and keeps nearly 2000 K. Thus the Gaussian broadening is about 0.07511 nm, slightly larger than the instrumental broadening. In fact, the Doppler broadening can be neglected compared with the instrumental broadening above in the simplified calculation. Figure 6 gives an example of Voigt fitting of H_β line. In the example, the Gaussian broadening (FWHM) is fixed at 0.07511 nm and the Voigt fitting is completed until the R-square R^2 (the larger R^2 is, the better the fitting is) maximizes. The best Voigt fitting gives a Lorentzian broadening (FWHM) of 0.12123 nm. The plasma pressure remains atmospheric (1 atm) due to the fact that the argon flows out of the quartz cavity through a hole (diameter $\approx$1 mm), while outer argon also flows into the cavity at a very low rate to prevent the air flowing into the cavity. Therefore, the van der Waals broadening is calculated to be 0.02700 nm (P = 1 atm, $T_{\rm g}$ = 2000 K). The Stark broadening is 0.09423 nm provided that the resonance and natural broadenings are ignored. The electron density $n_{\rm e}$ is inferred from Eq. (4) to be $3.03\times10^{14}\,{\rm cm}^{-3}$ and from Eq. (5) to be $2.73\times10^{14}\,{\rm cm}^{-3}$ corresponding to $T_{\rm e}$ of about 5600 K obtained by averaging the electron temperatures of different Ar I lines as shown in Fig. 5. Figure 7 shows the dependence of the electron densities inferred from these two equations on the input microwave power. The figure shows that the electron density $n_{\rm e}$ increases with the increase of the input microwave power and is on the order of $10^{14}\,{\rm cm}^{-3}$–$10^{15}\,{\rm cm}^{-3}$.

In conclusion, a novel microwave plasma source based inductive coupling window-rectangular resonator is developed. This plasma source can produce a definite volume of atmospheric argon microwave plasma. The argon plasma is at least in the partial local thermal equilibrium (pLTE). Its excitation temperature and electron temperature both increase from 5000 K to 8000 K with the increase of the input microwave power from 3 kW to 8 kW. The electron temperature is at most 400 K larger than the corresponding excitation temperature for every input power. The increase of the input power leads to the increase of the electron density and the density is on the order of $10^{14}\,{\rm cm}^{-3}$–$10^{15}\,{\rm cm}^{-3}$.

References

[1] Verhoff B, Harilal S S, Freeman J R, Diwakar P K and Hassanein A 2012 *J. Appl. Phys.* **112** 093303
[2] http://physics. nist.gov/PhysRefData/ASD/lines_form.html
[3] Sola A, Calzada M D and Gamero A 1995 *J. Phys. D: Appl. Phys.* **28** 1099
[4] Bussiere W, Vacher D, Menecier S and Andre P 2011 *Plasma Sources Sci. Technol.* **20** 045004
[5] Hofsaess D 1979 *At. Data Nucl. Data Tables* **24** 285
[6] Menart J, Heberlein J and Pfender E 1996 *J. Quant. Spectrosc. Radiat. Transfer.* **56** 377
[7] Menzel D H and Pekeris C L 1935 *Mon. Not. R. Astron. Soc.* **96** 77
[8] Laux C O, Spence T G, Kruger C H and Zare R N 2003 *Plasma Sources Sci. Technol.* **12** 125
[9] Yubero C, Garcia M C and Calzada M D 2006 *SpectroChim. Acta Part.* B **61** 540
[10] Vidal C R, Cooper J and Smith E W 1973 *Astrophys. J. Suppl.* **25** 37
[11] Zhu X M, Chen W C and Pu Y K 2008 *J. Phys. D: Appl. Phys.* **41** 105212
[12] Yubero C, Calzada M D and Garcia M C 2005 *J. Phys. Soc. Jpn.* **74** 2249